JJMIE

Volume 17, Number 3, September. 2023
ISSN 1995-6665
Pages 429– 440
https://doi.org/10.59038/jjmie/170312
Editor-in-Chief: Prof. Ali M. Jawarneh

Jordan Journal of Mechanical and Industrial Engineering

Vibration Feature Extraction and Artificial Neural Network-based Approach for Balancing a Multi-disc Rotor System

Ihsan A. Baqer*, WafaAbd Soud

University of Technology, Mechanical Engineering Department, Baghdad, Iraq.

Received 17 May 2023 *Accepted 18 Jul 2023*

Abstract

To ensure the design life of rotating systems, early detection of faults is crucial. Vibration analysis is a widely adopted technique for fault detection due to its popularity in the industry. This method utilizes signals to evaluate the state of the system and rectify faults when detected. In this study, time-domain vibration signals were processed using statistical features, such as the root mean square, peak-to-peak, kurtosis, and skewness. An artificial neural network was employed to assess an approach for detecting defects in an imbalanced system. To simulate the unbalance problem, a test rig consisting of a multi-disc rotor was utilized. Vibration data was collected using two vibration acceleration measurement boards (ADXL335) that were interfaced with an NI USB-6009 data acquisition device. Signal recording and processing for feature extraction purposes were performed using Matlab-Simulink software. The extracted vibration features were then used to train an artificial neural network model, which was subsequently experimentally tested using data that had not been previously utilized in the training phase. The results of this study demonstrate that the proposed approach is highly efficient in predicting and correcting unbalance faults within the rotor-bearing system.

Keywords: Artificial neural network, Rotating machines, Unbalance detection, Vibration features, Signal processing.

1. Introduction

Rotors are crucial components in rotary systems, such as compressors, pumps, and turbines, and the occurrence of self-excited vibration is one of the most common faults. Such vibration is produced due to the oscillation of an external load, such as an unbalanced load due to a cracked or bent shaft, which can lead to significant disturbances in the system [1, 2]. Many studies have been conducted to investigate the imbalance of rotational machines, which remains an open problem in technical investigation. Some investigations have focused on the relationship between unbalance and misalignment, and vibration analysis technique is a versatile method employed for machine analysis. Elman neural network and frequency-domain vibration analysis are used to diagnose faults due to unbalance conditions [3,4]. Various techniques, such as control theory, signal processing, and artificial intelligence (AI), particularly Artificial Neural Network (ANN) methods, have been used for monitoring and diagnosing the faults of mechanical systems [5, 6].

Unbalanced rotors can transmit generated forces to bearings and foundations, which can adversely affect the system and even influence nearby equipment. ANN with the plane separation technique is used to predict the location and magnitude of correction masses for balancing the rotor bearing system, where the Stodola-Green model is applied for rotating system modeling [5, 6]. There have been numerous investigations about rotating mechanical systems with AI techniques, particularly concentrated on minimizing vibration through appropriate bearing design [7]. The Genetic Algorithm (GA) technique is used to solve the optimization problem of minimizing bearing amplitudes. Another technique involves two consecutive optimization steps that minimize the ultimate value of rotor residual vibration [8].

The selection of the best inputs and the way of choosing the ANN parameters that ensure a compact structure and an extremely precise network are significant issues that face the utilization of ANN. Therefore, the genetic algorithm is utilized to select the most significant features of the full functionality database and optimize the ANN structure parameter, which is then trained and tested via chosen features of the measurement data [9]. The suggested technique is confirmed via simulations and experimentation associated with a double-disc rotor-bearing system through an optimum design to reduce the vibration level of the flexible rotor system [10].

The Fuzzy Logic approach is also used to evaluate the measurement data, where the measured vibration responses of the rotor over a long period are considered by defining unbalanced fuzzy sets. The unbalance condition of the rotating machine is determined through a defuzzification process [11]. Despite various methods employed to reduce or eliminate rotor unbalance, it is impossible to eliminate it entirely, and the unbalance can only be minimized to a residual extent. Hence, any other technique that can minimize the unbalance load to a further extent can be considered a substitute [12, 13].

* Corresponding author e-mail: ihsan.a.baqer@uotechnology.edu.iq.

In conclusion, the present study proposes a technique to predict unbalance mass, its location on the rotor, and its plane angle for balancing a multi-disc rotor system model using ANN without the need for any knowledge about the unbalancing magnitude, direction, and location for each disc of the rotor system. The proposed training process is based only on monitoring bearing vibration signals after processing with selective vibration statistical features and the geometrical information of the system. The study contributes to the body of knowledge on fault diagnosis and rotor balancing in rotating mechanical systems.

2. Materials and Methods

2.1. Description of System and Modeling

The rotating system under consideration consists of two primary discs, as depicted in Figure 1. Additionally, a third disc is interposed between the first and second discs. In order to introduce a corrective mass capable of balancing the rotating system, the second disc is mounted at a prescribed distance between the two bearings, while the first disc is mounted on the extended end of the shaft.

The industrial practice of offline balancing for rigid rotors is well-established. The rotor is considered a rigid shaft that lacks any elasticity during the balancing process. However, this technique is only suitable for low-speed rotors, where the assumption of a rigid rotor is valid, as a general rule for rotors running at less than 5000 rpm [14].

To achieve dynamic equilibrium in a multi-rotary disc system, mass redistribution is required through the addition or removal of machine elements. Rotational mass balance can be achieved by balancing a single rotating mass using a single mass rotating in the same plane, balancing a single rotating mass using two masses rotating in different planes, balancing several masses rotating in the same plane, or balancing several masses rotating in different planes. In this work, we considered the fourth case, where multiple masses rotating in different planes are transferred to a reference plane that passes through a point on the axis of rotation and is perpendicular to it. The resultant force and couple of magnitudes must be zero in the reference plane to achieve dynamic equilibrium.

For our proposed rotating system, we balanced multiple rotating masses in different planes to satisfy the above conditions. A corrective mass was mounted on the third disc plane to satisfy the first condition, while the location of the corrective mass satisfied the couple's balance. The corrective mass, corrective plane angle, and corrective mass location can be obtained using the following equations [15]. Firstly, we chose the reference plane at the second disc and found the distance of the first and third discs' planes from the reference plane as L_1 and L_c, respectively. Then, we determined the magnitude of the balancing masses using the steps provided.

The sum of the horizontal and vertical force components gives,

$$m_1 r_1 \cos\theta_1 + m_2 r_2 \cos\theta_2 + m_c r_c \cos\theta_c = 0 \quad (1)$$

$$m_1 r_1 \sin\theta_1 + m_2 r_2 \sin\theta_2 + m_c r_c \sin\theta_c = 0 \quad (2)$$

Squaring and adding eq. 1 to eq. 2 results in,

$$m_c = \frac{\sqrt{A_x^2 + A_y^2}}{r_c} \quad (3)$$

where, $A_x = m_1 r_1 \cos\theta_1 + m_2 r_2 \cos\theta_2$

and, $A_y = m_1 r_1 \sin\theta_1 + m_2 r_2 \sin\theta_2$

Then, the angle of the plane (θ_c) can be found by dividing ($\boldsymbol{A_y}$) by ($\boldsymbol{A_x}$), as in eq. 4

$$\theta_c = \tan^{-1}\frac{A_y}{A_x} \quad (4)$$

Then, to find the location of the corrective mass on the shaft, the second balance condition must be stratified. In other words, the sum of the horizontal and vertical couple components about the reference plane must be zero as follows.

$$m_1 r_1 L_1 \cos\theta_1 + m_c r_c L_c \cos\theta_c = 0 \quad (5)$$

$$m_1 r_1 L_1 \sin\theta_1 + m_c r_c L_c \sin\theta_c = 0 \quad (6)$$

Squaring and adding eq. 5 to eq. 6 results in,

$$L_c = \frac{m_1 r_1}{m_c r_c} L_1 \quad (7)$$

The primary objective of the mathematical model is to generate a set of balancing data (m_c, $L_c$and θ_c) for various virtual rotor system configurations, including parameters such as (m_1,m_2, r_1, r_2, L_1 ,L_2, θ_1 and θ_2). For each of the proposed system configurations, the system's vibration will be measured, and the resulting data will be processed using selective statistical features to prepare the artificial neural network (ANN) training data samples, as will be explained in later sections. This approach can be particularly useful for manufacturers of rotary machines, especially large machines such as turbines, compressors, marine crankshafts, and so on. These machines may experience mass loss due to operating conditions, and the balancing process requires shutting down the system and applying an expensive and complex procedure to correct the issue. The proposed approach, on the other hand, can detect the balancing data through vibration monitoring with artificial intelligence techniques, potentially reducing the time and effort involved in the balancing process.

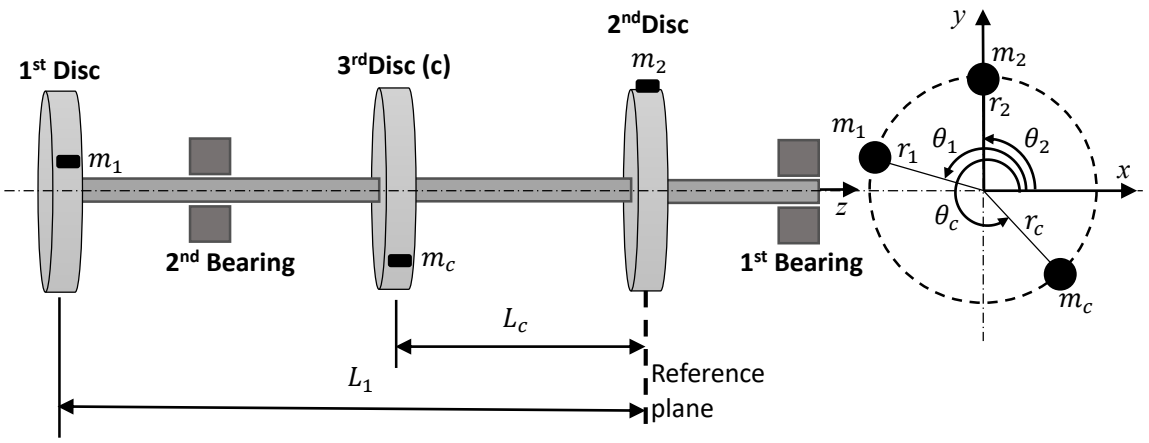

Figure 1. Multi-disc Rotating System

2.2. Architecture of Artificial Neural Network

The Artificial Neural Network (ANN) is a computational model inspired by the neuronal networks of the brain [16 , 17]. In this model, artificial neurons are connected to each other through synapse-like connections. The ANN consists of three primary layers: Input, Hidden, and Output layers, which collectively form a 3-layer network. The input layer contains the independent variables, which are processed in the hidden layer. The network weights (w) are estimated in the first step, followed by the transfer of data to the first hidden layer. The output of the first hidden layer is computed from the input data as described by [18]:

$$h_i^1 = S_i^1\left(b^1 + \sum_{j=1}^{p} w_{ij}^1 x_j\right) \quad (8)$$

where:

h_i^1: The output of the first hidden layer

S_i^1 : The activation function of the first hidden layer

b^1 : The bias of the first hidden layer

w_{ij}^1: The weights value of the first hidden layer

x_j : The input layer vector

j: The number of hidden layers

i: The number of elements (neurons) in each layer.

The activation function of the second hidden layer is applied to the weighted sum of the outputs from the first hidden layer. This is then used as input to the second hidden layer to compute the output of the neural network. The activation function used in the second hidden layer is typically chosen to be a non-linear function such as the sigmoid function. The output of the second hidden layer is then processed by the output layer, which computes the final output of the neural network. The output layer can have one or multiple nodes depending on the number of target variables to be predicted.

$$h_i^2 = S_i^2\left(b^2 + \sum_{j=1}^{m} w_{ij}^2 h_i^1\right) \quad (9)$$

where:

h_i^2: The output of the second hidden layer

S_i^2 : The activation function of the second hidden layer

b^2 : The bias of the second hidden layer

w_{ij}^2: The weights value of the second hidden layer

In the output layer, the process of forecasting or categorizing ends, and the outcomes are introduced with a small estimate error, and the output is computed as:

$$y = b^3 + \sum_{j=1}^{m} w_{ij}^3 h_i^2 \quad (10)$$

where:

y : The elements of the output layer

b^3 : The bias of the output layer

w_{ij}^2: The weights value of the output layer

In the described feedforward process, the activation function has an important role. This work uses the tan-sigmoid function in both the hidden layers, which is a widely dependent non-linear activation function.

$$S_i(x) = \frac{2}{1+e^{-2x}} - 1 \quad (11)$$

The objective of training a neural network is to find the optimal combination of weight and bias values, which is an iterative process. During each iteration, the backpropagation algorithm calculates a new set of weight and bias values that produce output values closer to the target values. The algorithm computes the error gradient and backpropagates the error through the network to update the weights and biases. The performance function used to evaluate the accuracy of the network is the mean square error (MSE), given by [19]:

$$E = \frac{1}{N}\sum_{i=1}^{N}\left(y_{d_i} - y_i\right)^2 \quad (12)$$

where:

N: The number of output data vectors

y_{d_i}: The desired output

y_i : The estimated output

It is important to note that Bayesian regularization is a type of regularization technique that helps prevent overfitting by adding a penalty term to the cost function. This penalty term is based on the prior probability distribution of the model's parameters, which is updated during the training process. Bayesian regularization can improve the generalization ability of the model, as it encourages the model to find a simpler solution that fits the data well. On the other hand, Levenberg-Marquardt is an optimization algorithm used to solve nonlinear least squares problems. It adjusts the step size during the iterative process, allowing it to converge to the minimum more efficiently than other algorithms. Both Bayesian regularization and Levenberg-Marquardt have been shown to be effective in improving the performance of artificial neural networks [20].

The architecture of the designed ANN model consists of 24 input nodes, 2 hidden layers with 10 neurons in each layer, and 3 neurons in the output layer. The input layer has 24 nodes because it represents the four vibration features extracted from the six acceleration components for the two bearings response. The two hidden layers with ten neurons in each were used to compute the weightings of the input variables and explore their influences on the target variables. The output layer comprises of three neurons that generate predictions for balancing data, namely m_c, L_c, and θ_c, for each of the three unbalanced scenarios.The performance goal was set to zero, and the training was stopped when the error reached an acceptable value. The number of epochs was limited to 1000. More information on the preparation of the input layer will be discussed later. The ANN modeling and simulation were conducted using MATLAB as shown in Figure 2.

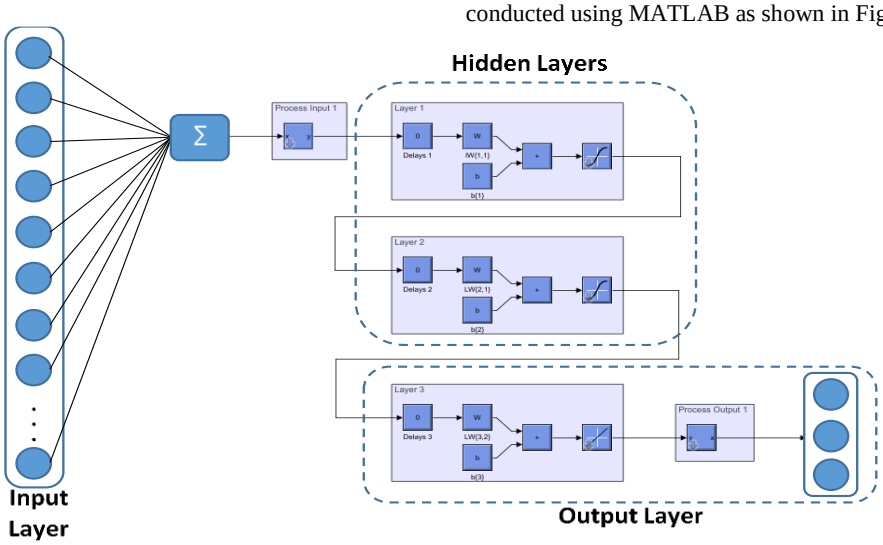

Figure 2. Architecture of the Artificial Neural Network

3. Experimental Work

3.1. Experimental Setup

From the fig.3, it can be inferred that the experimental setup includes a single-phase AC motor, a multi-disc rotor, pulleys, and two deep-groove bearings. The motor has a fixed rotational speed of up to 1350 rpm and a power rating of 0.75 kW with four slots to adjust the center distance with the rotor shaft.

The rotor shaft has a length of 600 mm, mounted on two deep-groove bearings, and the distance between the bearings is 400 mm. The outer diameter of each disc is 76 mm, with a weight of 890 g, and an additional unbalance mass of 10 g is mounted on the surrounding surface of the disc. The v-belt drive is used to drive the multi-disc rotor.

The bearing pedestals are mounted on steel base plates with rubber parts to insulate the produced vibrations.

The experimental setup includes three different diameters of driver pulleys (67 mm, 85 mm, and 112 mm) and three belt sizes of standard lengths (650 mm, 762 mm, and 800 mm) to produce different rotational speeds of 1461 rpm, 1832 rpm, and 2360 rpm, respectively.

3.2. Instrumentation and Sensory System

Vibration measurement is an important method for monitoring the condition of rotating machines, as it can detect and identify various types of faults such as misalignment, imbalance, bearing defects[21], and gear problems. By monitoring the vibration levels and analyzing the vibration signals, engineers can identify the root cause of the problem and take appropriate corrective actions before the machine fails or incurs significant damage. This can enhance the reliability of the machine, decrease maintenance expenses, and enhance safety [22]. The instrumentation used in this study includes a triple-axis acceleration board (ADXL330) fixed on bearing pedestals, which can measure both static gravitational acceleration and dynamic acceleration generated from vibration or shock. The sensor is equipped with a signal conditioning circuit that causes the sensor output to generate an analog voltage that corresponds to the level of vibration. Nevertheless, in this particular type of sensor, the primary origin of measurement noise is the sensor itself, which introduces Gaussian white noise [23]. The magnitude of the noise is directly related to the square root of the accelerometer's bandwidth, usually expressed in the range of μg/√Hz. In certain applications, such as various rotating systems, this noise may be disregarded when considering vibrations caused by large structures, as demonstrated in this study. The signals from the acceleration board are acquired through an NI-DAQ 6009 data acquisition device, which has eight analog input channels with a resolution of 14-bit and a maximum sampling rate of 48 kS/s. The DAQ device is controlled by Matlab-Simulink software to acquire the vibration signals, and the acquired signals for each unbalanced condition consist of 5000 samples of 5 s acquired at 1 kHz.Where, the use of Simulink can easily build models as block diagrams under a graphical user interface (GUI) environment by the aid of a comprehensive block library (see Fig.4). The acquired signals are then processed using vibration feature extraction functions such as RMS, Peak to Peak, Kurtosis, and Skewness to detect each case of imbalance. The rotational speed is measured using a tachometer.

4. Signal Processing and Analysis

4.1. VibrationFeature Extraction

Vibration signals in the time domain are commonly represented as a series of digital values for velocity and acceleration. Figure 5 illustrates the classification of vibration technology utilized in rotating machinery across various domains. These techniques are frequently employed to monitor the health of mechanical components and predict the occurrence of faults. Monitoring raw vibration signals may result in poor health evaluation due to the inherent noise present in these signals. Hence, statistical feature functions can be widely applied to vibration signals as an influential technique for feature extraction. In this work, statistical feature extraction has been employed as a data mining technique to ensure rotor unbalance monitoring accuracy. Four feature functions, namely root mean square, peak-to-peak, kurtosis, and skewness, were selected to reflect certain signal behaviors. Mechanical faults can manifest in vibration signals through two main effects: impulsive disturbance or an increase in overall vibration intensity. These characteristics are defined and formulated mathematically as follows:

The root mean square (RMS) represents a vibration feature used as a time analysis feature showing the power content of a vibration signal. Such a vibration feature is commonly used to detect an imbalance in the rotating machinery since it is very effective with this type of fault [24, 25]. Accordingly, the vibration signals are then treated by RMS and calculated in the following equation.

$$RMS = \sqrt{\frac{1}{N-1}\sum_{i=1}^{N}(x_i)^2} \tag{13}$$

Kurtosis is a dimensionless quantity that quantifies the deviation of a signal from the probability density function (PDF) and can be computed using the following equation.

$$Kurt = \frac{\frac{1}{N}\sum_{i=1}^{N}|x_i-\bar{x}|^4}{(\frac{1}{N}\sum_{i=1}^{N}|x_i-\bar{x}|^2)^2} \tag{14}$$

where $\bar{x}$ represent the mean of the signal.

Skewness measures the asymmetry in the probability distribution around its mean and represents the third distribution moment. This can be negative, positive, or zero, indicating left, right, or symmetric distributions. It can be computed as below.

$$Skw = \frac{\frac{1}{N}\sum_{i=1}^{N}|x_i-\bar{x}|^3}{\left(\sqrt{\frac{1}{N}\sum_{i=1}^{N}|x_i-\bar{x}|^2}\right)^3} \tag{15}$$

Peak to Peak amplitude provides the maximum excursion of the signal, which is commonly used when looking at displacement information and can be computed using the following equation.

$$PP = |max(x_i) - min(x_i)| \tag{16}$$

4.2. ANN Training Data

The current study employed a supervised training algorithm for the artificial neural network, whereby the inputs were derived from the training data comprising the four extracted vibration features of the six acceleration components for the two bearings' response. The computation of these features was carried out as follows:

$$n_i = feature(x_1); \tag{17}$$

$$n_i = feature(x_2); \tag{18}$$

$$n_i = \sqrt{feature(y_1)^2 + feature(z_1)^2}; \tag{19}$$

$$n_i = \sqrt{feature(y_2)^2 + feature(z_2)^2}; \tag{20}$$

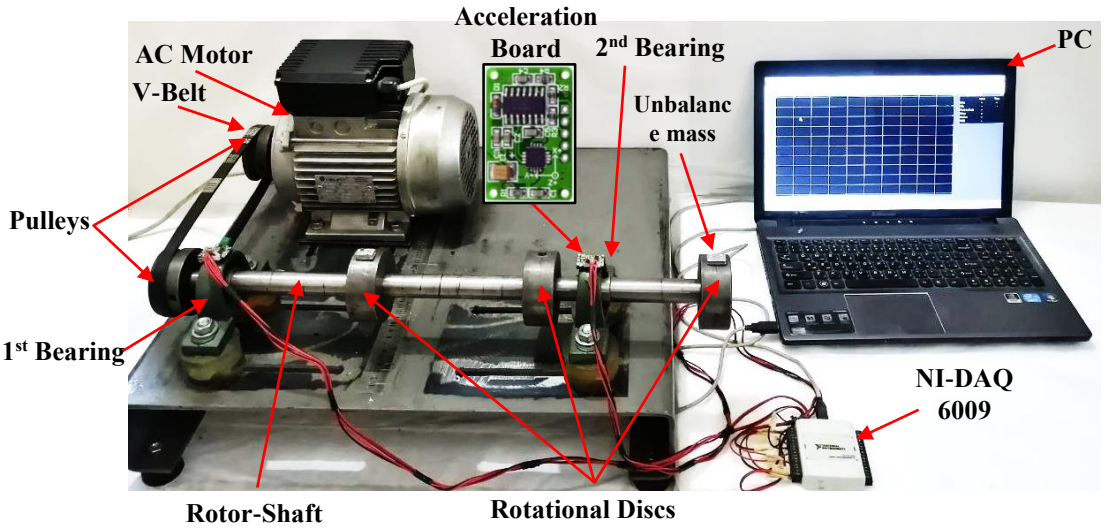

Figure 3. The experimental setup configuration

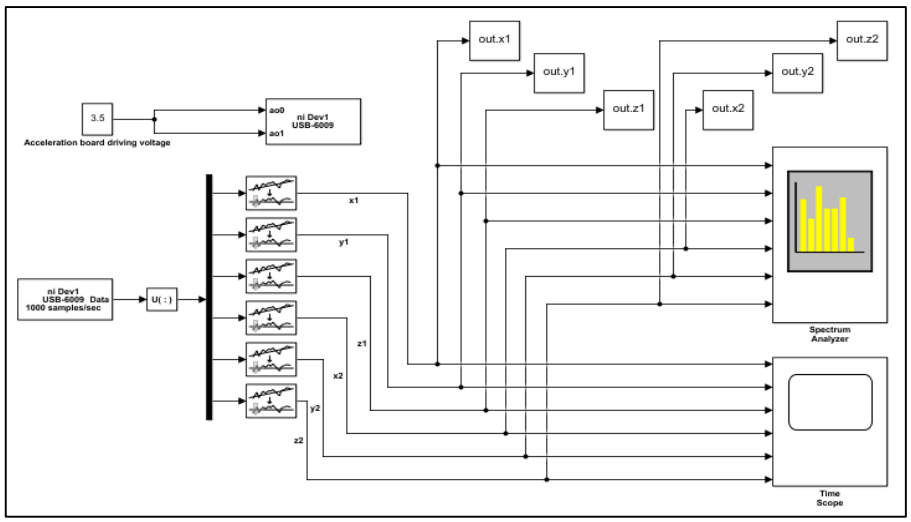

Figure 4. The block diagram of the Simulink model

$n_i = \tan^{-1}(feature(z_1)/feature(y_1))$; (21)

$n_i = \tan^{-1}(feature(z_2)/feature(y_2))$; (22)

where:

n_i represents the element of the input layer, and i refers to the element index in the input vector.

$feature$ represent the vibration extraction feature (RMS, PP, Kurt, Skw) since equations (17 - 22) will be repeated four times, one for each mentioned feature, as follows:

For i=1 to 6, the vibration feature is Root Mean Square

For i=7 to 12, the vibration feature is Peak-to-Peak

For i=13 to 18, the vibration feature is Kurtosis

For i=18 to 24, the vibration feature is skewness

(x_1, y_1,z_1 $and x_2$, y_2,z_2) are the measured acceleration components for both the first and second bearings, respectively.

For more clarification, Table (1) shows the input neurons in details.

It should be noted that in order to enhance the sensitivity of the artificial neural network for fault diagnosis, the resultant and direction of the vibration features are applied to the perpendicular acceleration components as shown in equations (19) to (22).

In this study, the correction mass (mc), its location with respect to the reference plane (Lc), and its plane angle (θc), those provided by equations (3) (4) and (7), are considered as the outputs of the artificial neural network (ANN).

In essence, the artificial neural network (ANN) undergoes training based on the generated vibration data from previously established balancing scenarios, where the outcomes of the mathematical model in these scenarios serve as the target output. The vibration characteristics are treated as input data. Consequently, the developed ANN relies solely on the measured vibration signal, without necessitating any information regarding unbalanced masses, including their quantity, location, and angular orientation on the rotor. During the training process, a range of unbalance defect parameters were simulated theoretically to compute these ANN outputs. Specifically, the additional masses (10g) were mounted on the first and second discs in various patterns (see Table (2)) to produce an unbalanced rotor system, and the dynamic response at both bearings was measured and recorded. This process was repeated 32 times to train the ANN on a range of alternative balancing processes. The resulting ANN was then able to balance the rotor system without prior knowledge of the specific unbalance defect parameters. The process of preparing the ANN training data is detailed in the flowchart presented in Figure 6.

To avoid overtraining in an Artificial Neural Network (ANN), the implementation of cross-validation techniques is necessary. This involves splitting the dataset into training and testing sets, with the testing set being used to monitor the model's performance during training.

Table 1. The details of input layer elements

Input Neurons	Function
1	$RMS(x_1)$
2	$RMS(x_2)$
3	$\sqrt{RMS(y_1)^2 + RMS(z_1)^2}$
4	$\sqrt{RMS(y_2)^2 + RMS(z_2)^2}$
5	$\tan^{-1}(RMS(z_1)/RMS(y_1))$
6	$\tan^{-1}(RMS(z_2)/RMS(y_2))$
7	$PP(x_1)$
8	$PP(x_2)$
9	$\sqrt{PP(y_1)^2 + PP(z_1)^2}$
10	$\sqrt{PP(y_2)^2 + PP(z_2)^2}$
11	$\tan^{-1}(PP(z_1)/PP(y_1))$
12	$\tan^{-1}(PP(z_2)/PP(y_2))$
13	$KURT(x_1)$
14	$KURT(x_2)$
15	$\sqrt{KURT(y_1)^2 + KURT(z_1)^2}$
16	$\sqrt{KURT(y_2)^2 + KURT(z_2)^2}$
17	$\tan^{-1}(KURT(z_1)/KURT(y_1))$
18	$\tan^{-1}(KURT(z_2)/KURT(y_2))$
19	$SKEW(x_1)$
20	$SKEW(x_2)$
21	$\sqrt{SKEW(y_1)^2 + SKEW(z_1)^2}$
22	$\sqrt{SKEW(y_2)^2 + SKEW(z_2)^2}$
23	$\tan^{-1}(SKEW(z_1)/SKEW(y_1))$
24	$\tan^{-1}(SKEW(z_2)/SKEW(y_2))$

Table 2. Patterns of unbalanced defects parameters and disc distribution varying

		θ_1 (deg)	θ_2 (deg)	m_1 g	m_2 g	L_1 mm
Patterns	**1st**					
	.	**0**	**0**			**180**
	.	.	.			.
	.	.	.	**10**	**10**	.
	.	.	.			.
	.	**180**	**180**			**480**
	32th					

5. Results and Discussion

5.1. Vibration Monitoring and Analysis

Vibration monitoring and analysis is a widely-used technique for detecting faults in mechanical systems, particularly in the case of unbalance faults. In this study, vibration signals in the frequency domain were analyzed to monitor the system under various unbalanced conditions.

The obtained vibration signals were first analyzed using the power spectrum analyzer in Matlab-Simulink software [26]. An unbalance fault produces a peak of 1X(peak at the excitation frequency) amplitude in the FFT spectrum, while other faults can also produce harmonics with peaks of 1x amplitude. From Figures 7 to 9, it can be observed that significant peaks in the signal spectrum, specifically at rotational speed frequencies of 25 Hz, 30.5 Hz, and 39.33 Hz, respectively, have predominant 1X components, indicating the presence of unbalance. Comparison of these peaks before and after rotor balancing clearly shows a reduction in RMS of acceleration magnitude.

Another notable peak occurs at a frequency of 100 Hz, which is generated in the AC motor and transmitted through the base plate to the rotor bearings. AC motor problems often cause high vibration at twice the electrical line frequency of the electrical grid (50 Hz) [27].

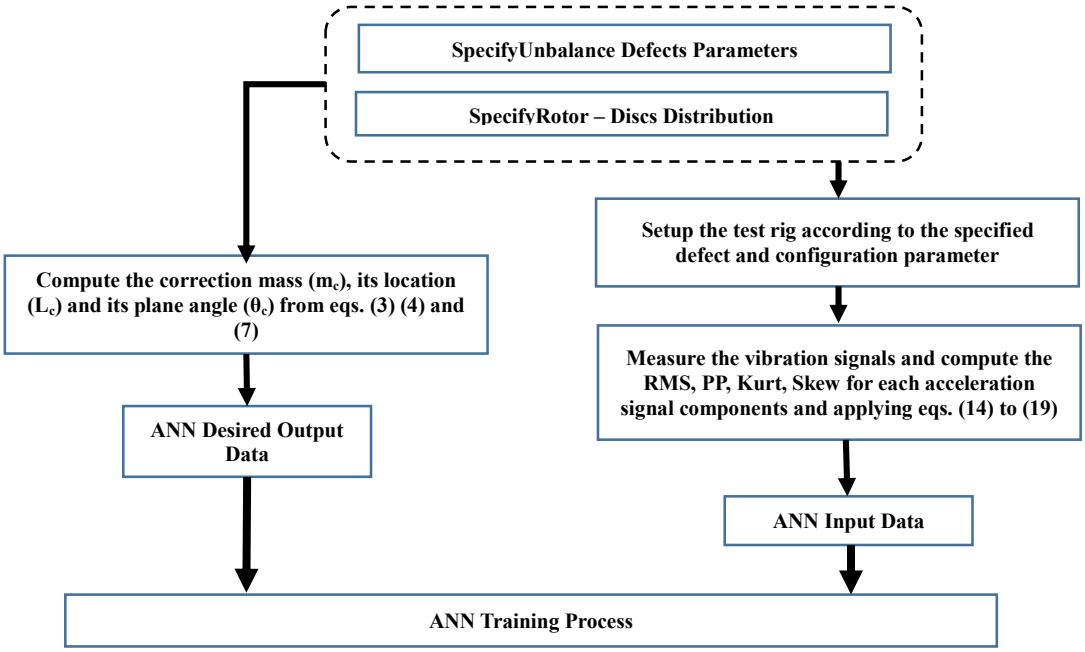

Figure 6. The flowchart of the ANN training data preparation process.

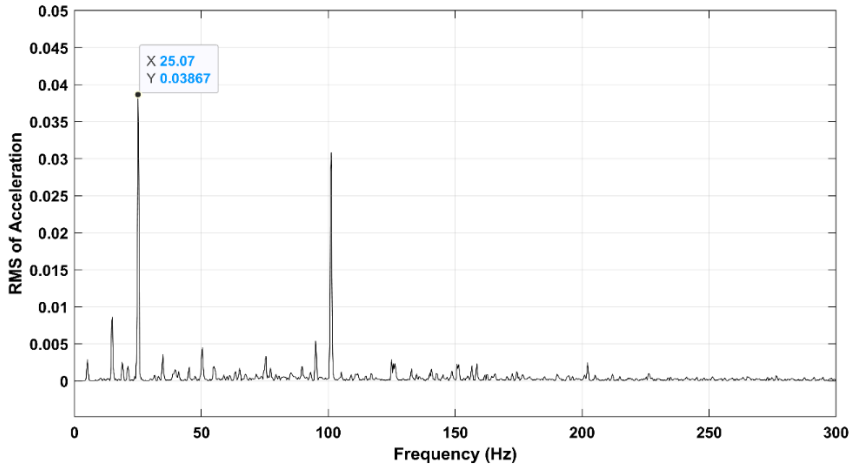

(a)

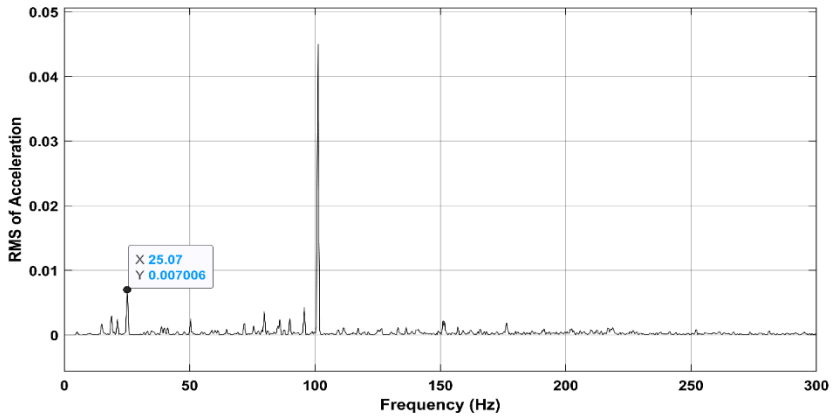

(b)

Figure 7. Spectrum of Y-component vibration signal at the 2nd bearing for (a) unbalanced and (b) balanced conditions under rotational speed of 1461 rpm.

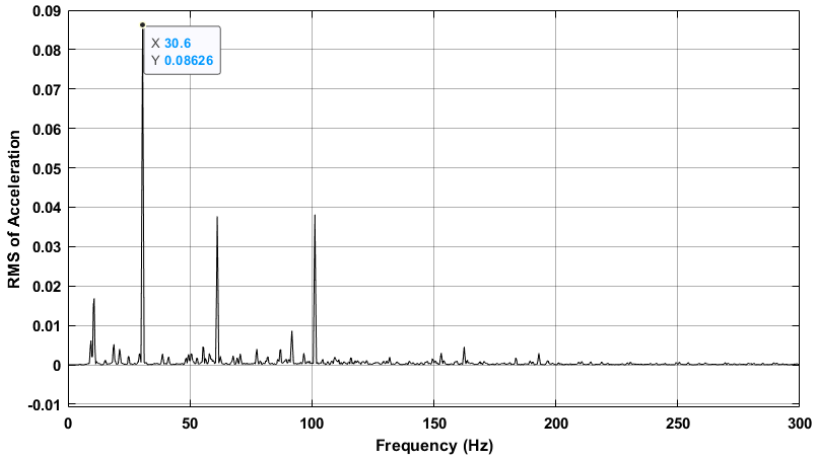

(a)

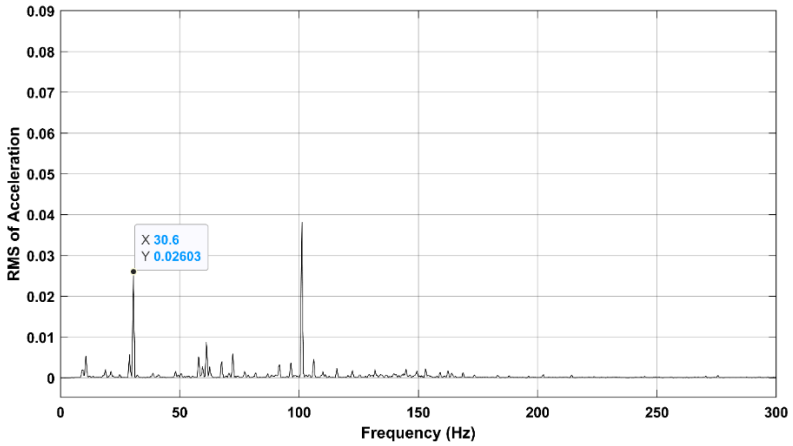

(b)

Figure 8. Spectrum of Z-component vibration signal at the 1st bearing for (a) unbalanced and (b) balanced conditions under rotational speed of 1832 rpm.

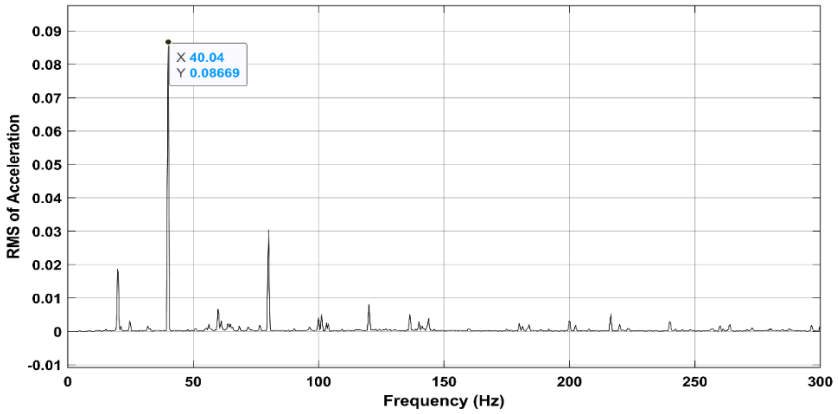

(a)

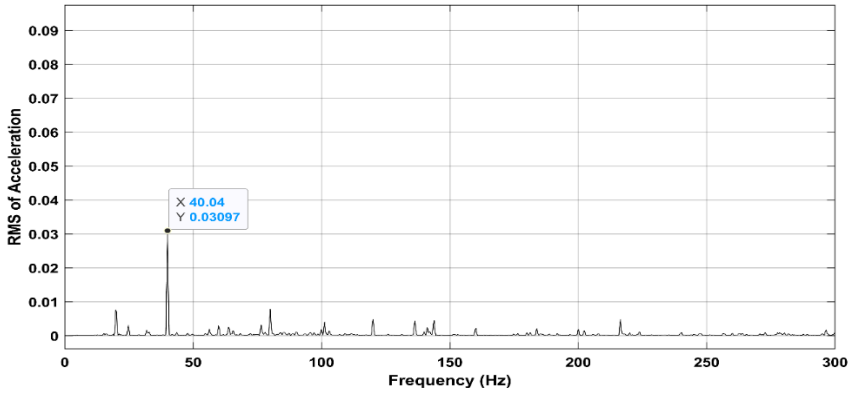

(b)

Figure 9. Spectrum of X-component vibration signal at the 1st bearing for (a) unbalanced and (b) balanced conditions under rotational speed of 2360 rpm.

To facilitate fault detection, vibration feature extraction has been employed to create a database for the fault recognition technique. In this section, we present and discuss selected results obtained under specific operational conditions. Root mean square (RMS), peak-to-peak (PP), kurtosis (Kurt), and skewness (Skw) with respect to rotational speed for the vibration signals of both bearings under both balanced and unbalanced conditions are presented in Figures 10 to 13. These features were selected due to their effectiveness in characterizing vibration signals and identifying fault occurrence.

In general, from the statistical features presented in Figures 10 to 13, several observations can be summarized as follows:

1. The observed increase in the root mean square (RMS) and peak-to-peak (PP) features of the vibration signals in the unbalanced condition, as compared to the balanced case, can be attributed to the heightened energy generated by vibration due to the presence of unbalance. The RMS and PP features are closely related to the intensity of the vibration signal level, which is why their values are increased in the presence of unbalance.
2. The kurtosis feature, which measures the sharpness of the peak of a distribution, has been observed to increase in the unbalanced case compared to the balanced operation at both bearings. This indicates that the level of vibration peaks has increased due to the occurrence of an unbalanced fault.
3. Based on the extracted skewness feature values, it can be noted that the unbalanced condition results in negative skewness values in the vibration signals, while the balanced operation exhibits positive skewness feature values.

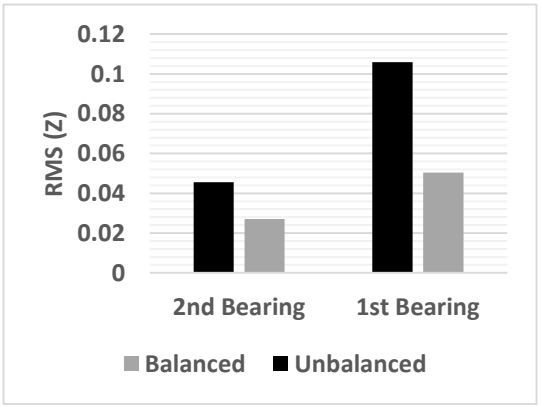

Figure 10. The RMS of Z-component of vibration signal on both 1st and 2nd bearings under balanced and unbalanced case with a rotational speed of 1832 rpm

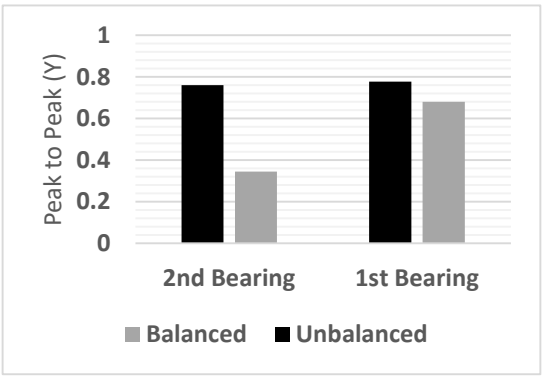

Figure 11. The Peak-to-Peak of Y-component of vibration signal on both 1st and 2nd bearings under balanced and unbalanced case with a rotational speed of 2360 rpm

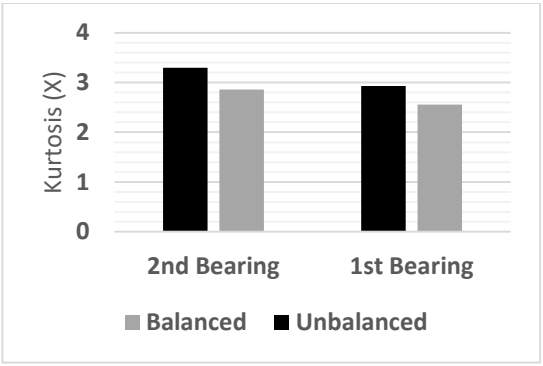

Figure 12. The Kurtosis of X-component of vibration signal on both 1st and 2nd bearings under balanced and unbalanced case with a rotational speed of 1461 rpm

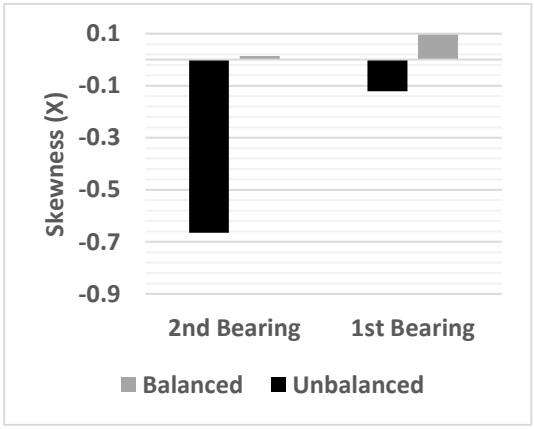

Figure 13. The Skewness of X-component of vibration signal on both 1st and 2nd bearings under balanced and unbalanced case with a rotational speed of 1461 rpm

5.2. ANN Training Results

The efficacy of various ANN architectures was evaluated by employing ten distinct training algorithms. Based on the comparison results presented in Table (3), the Bayesian Regularization (BR) algorithm was chosen, as it produced the lowest mean square error between the outputs and targets. Moreover, the optimal ANN architecture was determined to comprise two hidden layers, each comprising ten neurons.

Table 3. The Performance of ANN with Varying of Training Algorithm.

Training Algorithm	Mean Squared Error
Bayesian Regularization algorithm	2.43E-27
Levenberg-Marquardt algorithm	5.85E-27
BFGS Quasi-Newton algorithm	63.7
RProp algorithm	0.115
Scaled Conjugate Gradient algorithm	0.503
Conjugate Gradient with Beale-Powell Restarts algorithm	0.27
Conjugate Gradient Backpropagation with Fletcher-Reeves Restarts algorithm	0.21
Conjugate Gradient with Polak-Ribiere Restarts algorithm	0.414
One Step Secant algorithm	3.6
Gradient Descent with Momentum & Adaptive LR algorithm	197

After randomly selecting 70% of the available 320 data samples for training purposes, the remaining 30% was reserved for testing the process. During each training epoch, the weights and bias quantities of the neural network were adapted until the best performance was achieved. This process continued until the neural network reached its optimal performance after 73 epochs, as demonstrated in Figures 14 to 16.

In Figure 14, it can be observed that the neural network achieved a minimum mean square error of 2.43 E-27. Figure 15 shows that the majority of error values are clustered around a single error value of -7.1E-15, indicating the network's ability to generalize and effectively handle different unbalance cases, while taking into account the geometry parameters of the rotor-discs system. The convergence of the regression output and target results is evident from Figure 16, which is a testament to the network's robust performance.

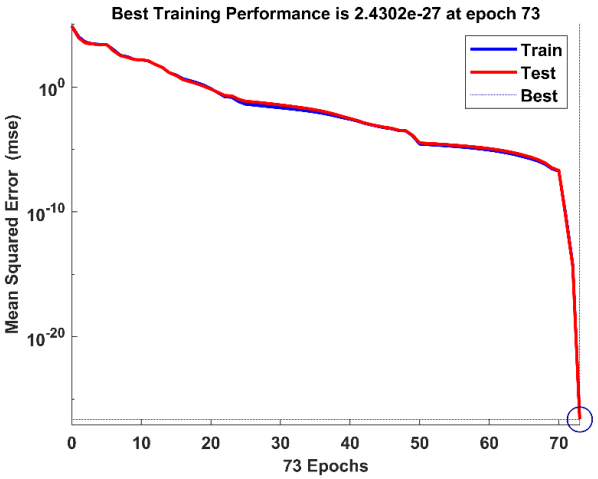

Figure 14. The Performance of ANN.

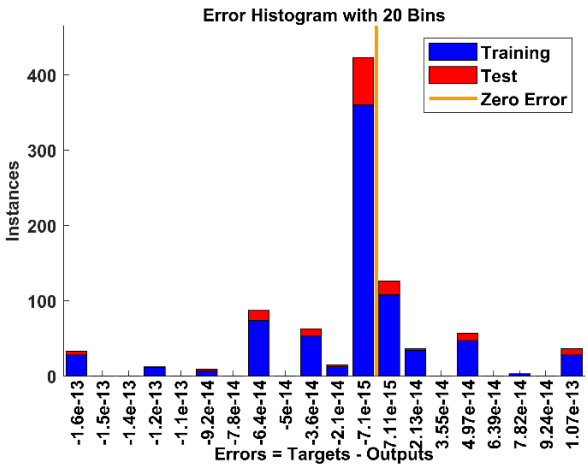

Figure 15. The Error Histogram of the ANN

5.3. ANN Testing Results

In order to assess the generalization performance of the ANN, the model was tested on multiple unseen rotor system configurations. This was achieved by varying the distances between discs, the angle of the unbalance mass plane in both the first and second discs, and the rotational speed. The resulting vibration responses were processed using vibration extraction features based on equations 17 to 22, and the ANN was used to predict the corrective mass (mc), its location on the rotor (Lc), and its plane angle (θc). The simulation results are presented in Fig. 17.

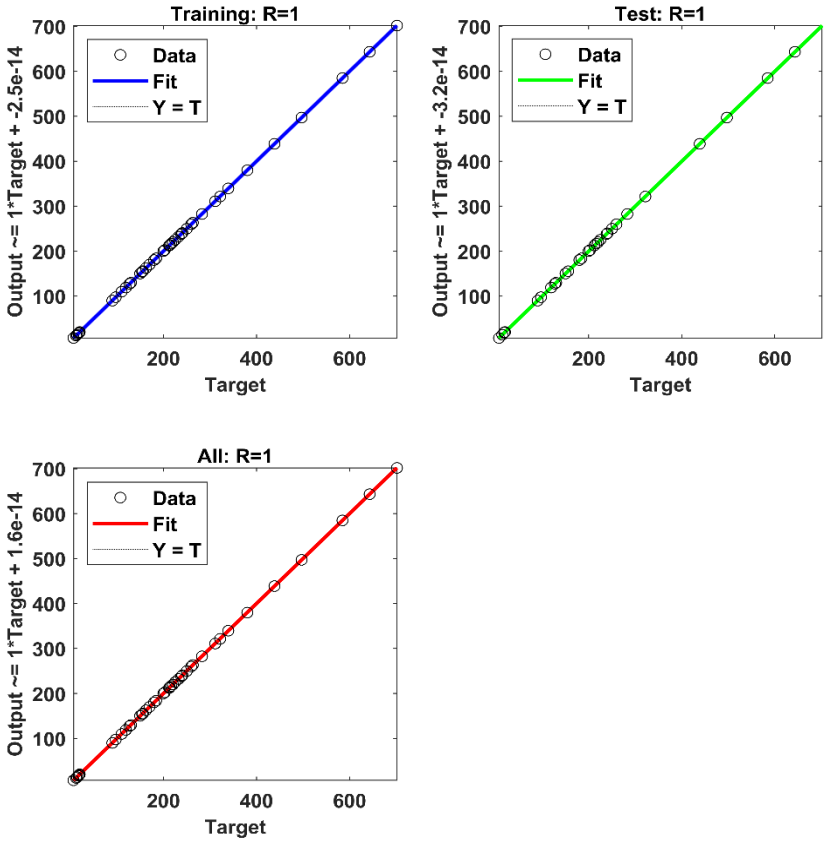

Figure 16. The regression between Outputs and targets of the ANN

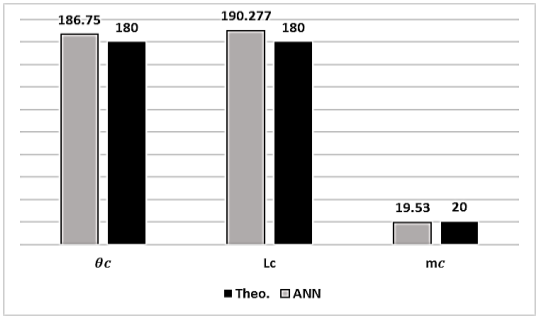

Figure 17. Comparison between Balancing Parameters Predicted by ANN and that Computed Theoretically

The findings presented in Figure 17 demonstrate that the artificial neural network (ANN) is capable of accurately predicting the corrective balancing parameters (m_c, L_c, and θ_c) based on the system's vibration response. Notably, the ANN obviates the need for knowing the unbalance masses and plane angles on each disc, as required by theoretical prediction methods. In order to further validate the ANN's performance, experimental tests were conducted by applying corrective mass and its plane angle on the third disc, effectively designating it as disc c to balance the system. The results of the vibration response before and after the balancing process at a rotational speed of 2360 rpm for both first and second bearings are illustrated in Figures 18 and 19.

The figures presented in Figs. 18-19 demonstrate the discernible impact of balancing on the vibration response, particularly the measured response on the second bearing, which shows a greater reduction than that on the first bearing. This can be attributed to the proximity of the second bearing to disc (c) in comparison to the position of the first bearing. Specifically, the distance between disc (c) and the second bearing was 180 mm, while the distance to the first bearing was 220 mm. Additionally, it is worth noting that the first bearing is situated closer to the sheave driven by the AC motor and hence, is more susceptible to its vibrations in comparison to the second bearing [28].

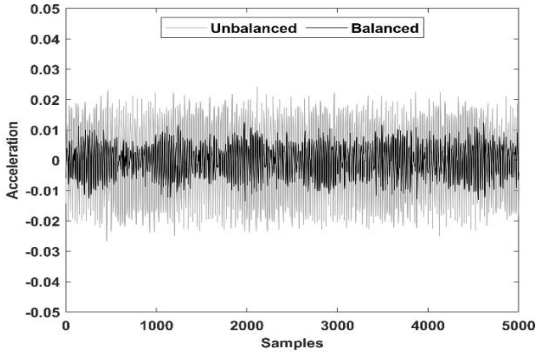

Figure 18. Comparison between the vibration response of first bearing in Z-Direction before and after Balancing.

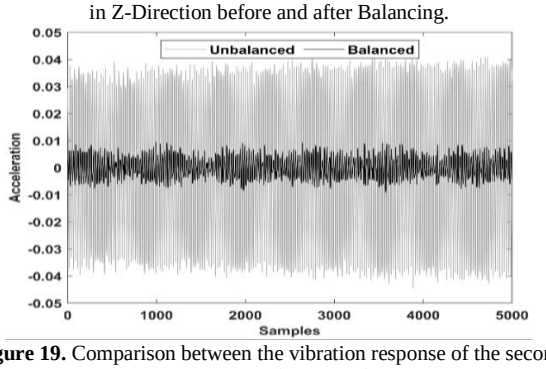

Figure 19. Comparison between the vibration response of the second bearing in Z-Direction before and after Balancing

6. Conclusion

In the field of rotating systems, minimizing vibrations generated by unbalanced masses is a crucial goal. Accurately predicting the values of the unbalance mass, its position on the rotor, and its angular location is necessary to eliminate these vibrations. To achieve this, an experimental test rig was constructed using an AC motor, pulleys, and a V-belt. A data acquisition system was established using two acceleration boards, an NI USB-6009 data acquisition device, and Matlab Simulink software. Vibration extraction features were employed to process the vibration signals and build the ANN training database. These features enhance fault recognition capabilities beyond other balancing techniques that rely solely on the acquired vibration signal's amplitude. An ANN model was developed and trained using various training algorithms, with the Bayesian Regularization (BR) algorithm being selected due to its superior performance. The ANN was optimized using a two-hidden-layer structure, with ten neurons in each layer. The data set was divided into 70% for training and 30% for testing. The ANN was deemed optimal when the mean square error reached 2.43E-27 during the 73rd epoch. The testing results of the ANN showed high accuracy and excellent predictive ability in comparison to the results achieved in Ref. [3] (MSE = 0.0471 after 996 epochs). The developed ANN model can be further developed for active control purposes by simultaneously monitoring, detecting, and correcting faults.

Statements and Declarations

We wish to confirm that there are no known conflicts of interest associated with this publication, and there has been no significant financial support for this work that could have influenced its outcome.

References

[1] M. Gohari and A. Kord, “Unbalance Rotor Parameters Detection Based on Artificial Neural Network,” International Journal of Acoustics and Vibration, vol. 24, no. 1, 2019, pp. 113-118. https://doi.org/10.20855/ijav.2019.24.11272.

[2] M. Kalkat, S. Yıldırım and I. Uzmay, “Rotor Dynamics Analysis of Rotating Machine Systems Using Artificial Neural Networks,” International Journal of Rotating Machinery, vol. 9, 2003, pp. 255-262.https://doi.org/10.1080/10236210390202874.

[3] S. Sendhilkumar, N. Mohanasundaram, M. Senthilkumar and S. N. Sivanandam, “Elman Neural Network for Diagnosis of Unbalance in a Rotor-Bearing System,” International Journal of Mechanical and Mechatronics Engineering, vol. 10, no. 3, 2016, pp. 613-617.https://doi.org/10.5281/zenodo.1124759.

[4] Nawafleh MA, Al-Kloub N, Tarawneh M, Younesd RM. "Reduction of vibration of industrial equipments". Jordan Journal of Mechanical and Industrial Engineering. Vol.4, no.4 .2010, pp:495-502.

[5] F. L. Santos, M. L. M. Duarte, M. T. C. deFaria and A. C. Eduardo, “Balancing of a rigid rotor using artificial neural network to predict the correction masses,” ActaScientiarum Technology, vol. 31, no. 2,2009, pp. 151-157. https://doi.org/10.4025/actascitechnol.v31i2.3912.

[6] A. Eduardo, F. Santos and M. Duarte, “Balancing Methodology of a Rigid Rotor Using Artificial Neural Network,” in 18th International Congress of Mechanical Engineering, ABCM, 2005, OuroPreto, MG.

[7] H. Taplak, S. Erkaya and İ. Uzmay, “Passive balancing of a rotating mechanical system using genetic algorithm,” ScientiaIranica, vol. 19, no. 6, 2012, pp. 1502–1510. https://doi:10.1016/j.scient.2012.10.026.

[8] J. Yao, F. Yangb, Y. Su, F. Scarpa and J. Gao, "Balancing optimization of a multiple speeds flexible rotor," Journal of Sound and Vibration, vol. 480, 2020, pp. 115405.https://doi.org/10.1016/j.jsv.2020.115405.

[9] T. Han, B.-S. Yang, W.-H. Choi and J.-S. Kim, "Fault Diagnosis System of Induction Motors Based on Neural Network and Genetic Algorithm Using Stator Current Signals," International Journal of Rotating Machinery, 2006, pp. 1-13. https://doi.org/10.1155/IJRM/2006/61690.

[10] Z. Longxi, J. Shengxi and H. Jingjing, "Numerical and Experimental Study on the Multiobjective Optimization of a Two-Disk Flexible Rotor System," international Journal of Rotating Machinery, 2017, pp. 1-10. https://doi.org/10.1155/2017/9628181.

[11] V. N. Carvalho, B. F. Resende, A. D. Guerra, A. A. Cavalini and V. Steffen, "Robust balancing approach for rotating machines based on fuzzy logic," Journal of Vibration and Acoustics, vol. 140, 2018, pp. 051018-1:9.https://doi.org/10.1115/1.4039801.

[12] W. A. Oke, M. A. Abido and T. B. Asafa, "Balancing of flexible rotors based on evolutionary algorithms," Mechanics & Industry, vol. 16, 2015. https://doi.org/10.1051/meca/2015013.

[13] Y. Zhang, M. Li and Y. Hu, "Model-based Balancing Method of Rotors using Differential Evolution Algorithm," in IOP Conf. Series: Materials Science and Engineering, Sanya, China, 2020. https://doi.org/10.1088/1757-899X/751/1/012046.

[14] S. Zhou and J. Shi, "Active Balancing and Vibration Control of Rotating Machinery: A Survey," Shock and Vibration Digest, vol. 33, no. 4, 2001, pp. 361-371.http://doi.org/10.1177/058310240103300501.

[15] McMillan, R.B., "Rotating Machinery, Practical Solutions to Unbalance and Misalignment", (1st Edition). River Publishers, 2004.https://doi.org/10.1201/9781003151142.

[16] Anitha J, Dasa R, Pradhan MK. "Multi-objective optimization of electrical discharge machining processes using artificial neural network". Jordan Journal of Mechanical and Industrial Engineering. Vol.10, no.1, 2016, pp:11-18.

[17] I. Jalham, "A Two-stage Artifitial Neural Network Model to Predict the Shrinkage of a Polystyrene Matrix Reinforced withSilica Sand and Cement", Jordan Journal of Mechanical and Industrial Engineering. Vol.5, no.3, 2011, pp:255-259.

[18] M. Kayri, "Predictive Abilities of Bayesian Regularization and Levenberg–Marquardt Algorithms in Artificial Neural Networks: A Comparative Empirical Study on Social Data," Mathematical and Computational Applications, vol. 21, no. 20, 2016, pp. 1-11.https://doi.org/10.3390/mca21020020.

[19] Ismail FB, Al-Bazi A, Al-Hadeethi RH, Victor M. "A Machine Learning Approach for Fire-Fighting Detection in the Power Industry". Jordan Journal of Mechanical and Industrial Engineering. Vol.15, no.5, 2021; pp:475-482.

[20] Asmael M., Fubara O.T., and Nasir T., "Prediction of SpringbackBehavior of Vee Bending Process of AA5052 Aluminum Alloy Sheets Using Machine Learning", Jordan Journal of Mechanical and Industrial Engineering. Vol.17, no.1, 2023; pp:1-14.

[21] Rao VV, Ratnam C. "Estimation of Defect Severity in Rolling Element Bearings using Vibration Signals with Artificial Neural Network". Jordan Journal of Mechanical and Industrial Engineering. Vol.9, no.2, 2015; pp:113-120.

[22] R. Srilakshmi, C. Ratnam and V. V. Rao, "A Review on Fault Detection, Diagnosis and Prognosis, in Vibration Measurement through Wavelets on Machine Elements," International Journal of Applied Engineering Research, vol. 14, no. 2, 2019, pp. 547-555.

[23] J. Barman and D. Hazarika, "Linear and Quadratic Time–Frequency Analysis of Vibration for Fault Detection and Identification of NFR Trains," IEEE Transactions on Instrumentation and Measurement, vol. 69, no. 11, 2020, pp. 8902-8909,.https://doi.org/10.1109/TIM.2020.2998888.

[24] S. Riaz, H. Elahi, K. Javaid and T. Shahzad, "Vibration Feature Extraction and Analysis for Fault Diagnosis of Rotating Machinery-A Literature Survey," Asia Pacific Journal of Multidisciplinary Research, vol. 5, no. 1, 2017, pp. 103-110.

[25] Samhouri, M., A. Al-Ghandoor, S. Alhaj Ali, I. Hinti, and W. Massad. "An intelligent machine condition monitoring system using time-based analysis: neuro-fuzzy versus neural network." Jordan Journal of Mechanical and Industrial Engineering,vol.3, no. 4 ,2009, pp: 294-305.

[26] Mais, Jason. "Spectrum analysis: the key features of analyzing spectra." SKF USA, Inc, 2002.

[27] Mohamed, Karim Abdel-Hakam, Galal Ali Hassaan, and Adel A. Hegazy, "Induction Motor Electrical Fault Diagnosis by a Fundamental Frequency Amplitude using Fuzzy Inference System.", International Journal of Recent Engineering Science, vol.2, issue.6, 2015, pp.15-24.

[28] K. Ágoston,"Studying and Measuring System for Motor Base Unbalance," in 13th International Conference Interdisciplinarity in Engineering, TarguMures, Romania, 2020.http://doi.org/10.1016/j.promfg.2020.03.057.